Real-space Calculation Method for Electronic Structure and Transport Property of Nanoscale Devices

University of Tsukuba & JST-PRESTO Tomoya Ono/小野倫也

Contents

Evolutions of DFT calculation and computers

exa, zetta, yotta mechines?

Kei (2011)
[88,128cpu/10.8Tflops]

Several projects to develop real-space code are lounched (Late 2000s)
GPAW/Denmark & Finland(2005), RSDFT/Japan(2006), JüRS/Germany(2007)

Textbook for real-space calculation method (2005)

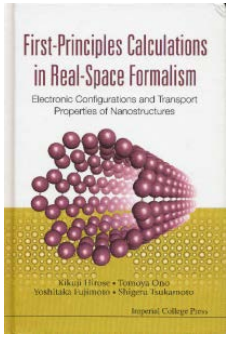

K. Hirose, TO, Y. Fujimoto, S. Tsukamoto
(Imperial College Press, London, 2005)

Earth simulator(2002)
[5,120cpu/41.0Tflops]

Double-grid method (TO, K. Hirose)
(Prescription for egg box effect)(1999)

CP-PACS(1996)
[2,048cpu/614Gflops]
massively parallel computer

Real-space finite-difference method
(Chelikowsky) (1994)

NEC SX-3(1989)
[4cpu/22.0Gflops]1st shared mem. comp. in JPN

Car-Parrinello Molec. Dyn. (1985)

FACOM VP-200(1982)
[1cpu/571Mflops]1st vector comp. in JPN

Pseudopotentials (Hamman et al.) (1981)

Density functional theory
(Hohenberg & Kohn) (1964)

Real-space finite-difference (RSFD) method

The grand-state electronic structure is obtained by solving the Schrödinger (Kohn-Sham) equation

$$\left(-\frac{1}{2}\nabla^2 + V(r)\right)\psi_i(r) = \varepsilon_i \psi_i(r)$$

The RSFD method is:

- the space is divided into equal-spacing grid points,
- the wave function and potential are defined at the grid points,
- the kinetic operator is approximated to a finite-difference formula, e.g.,

$$-\frac{1}{2}\frac{d^2}{dz^2}\psi(z_k) \approx -\frac{\psi(z_{k+1}) - 2\psi(z_k) + \psi(z_{k-1})}{2h_z^2}$$

- no use of a basis-function set

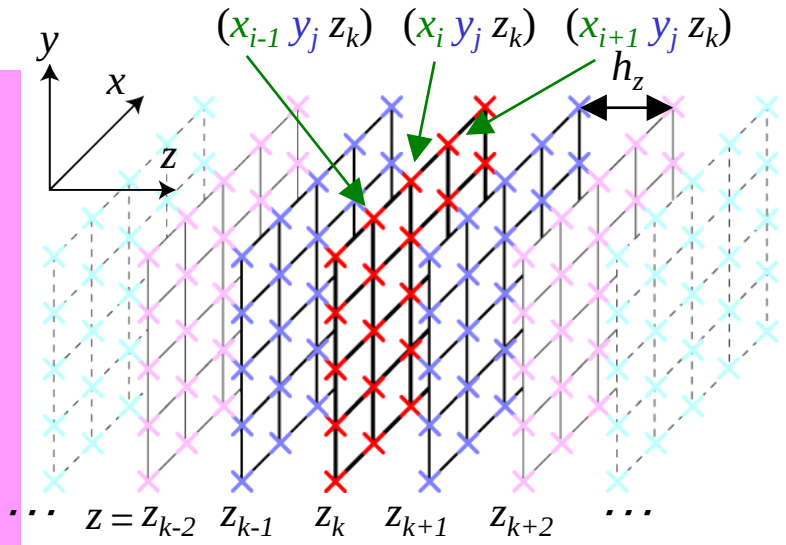

Wave function ψ_{ijk} is defined at grid point $(x_i\ y_j\ z_k)$

References of the RSFD approach, .e.g.,

J. R. Chelikowsky *et al.*, Phys. Rev. B **50**, 11355 (1994),
T. Ono & K. Hirose, Phys. Rev. Lett. **82**, 5016 (1999),
T. Ono & K. Hirose, Phys. Rev. B **72**, 085105 (2005),
T. Ono *et al.*, Phys. Rev. B **82**, 205115 (2010).

Advantages of RSFD 1

Advantageous on massively parallel computers.

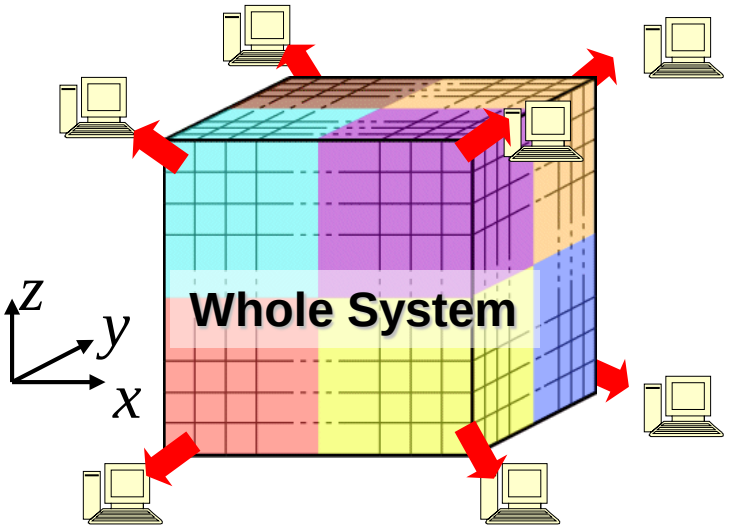

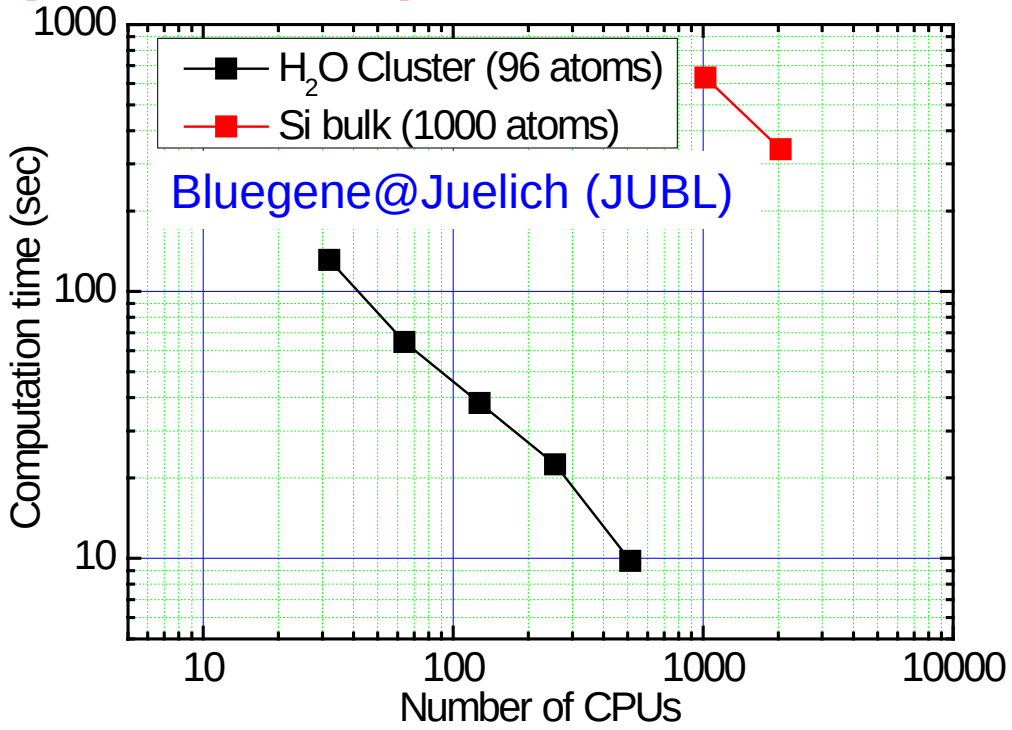

Example: Peapod C_{180}@(20,0)CNT (500 C atoms/supercell)

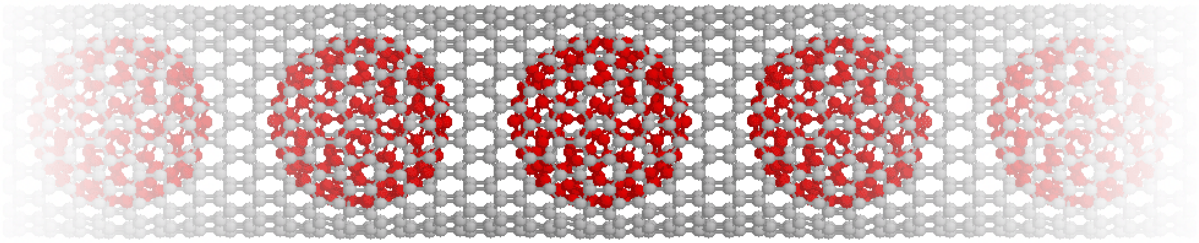

Computed by 2048CPUs of JUBL

Φ_{CNT}: +4% Φ_{C180}: -6%(lateral), +1%(longitudinal)
by encapsulating fullerene.

Advantages of RSFD 2

Arbitrary boundary condition is available.

Conventional plane-wave method

Repeated slab model

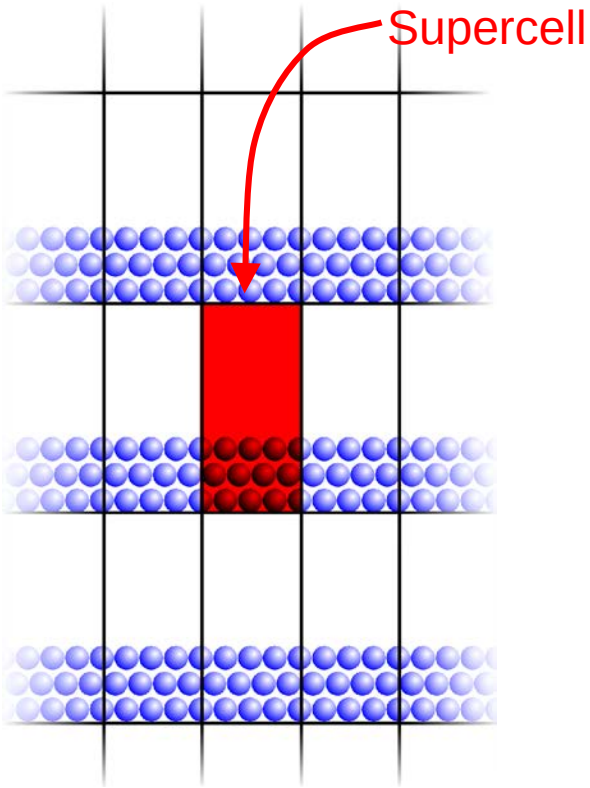

RSFD method

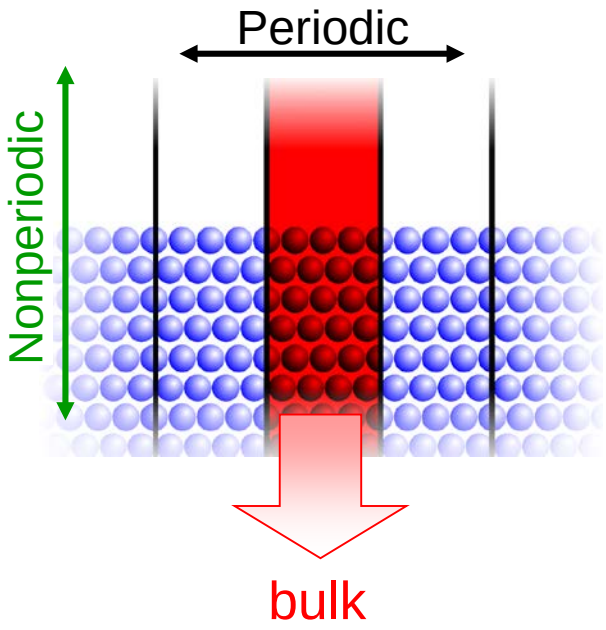

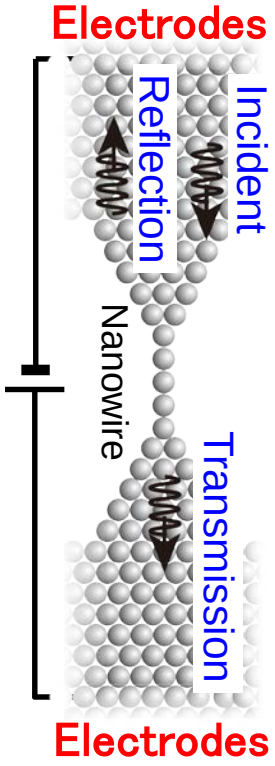

Computational model for transport calculation

The boundary condition infinitely continuing to bulk is available.

Computational Code RSPACE

***Ab initio* molecular-dynamics simulation program based on Real-SPACE finite-difference method**

T. Ono (U. of Tsukuba) in collaboration with
S. Tsukamoto (FZJ), Y. Egami (Hokkaido U.), S. Iwase (Osaka U.)

- Real-space finite-difference method with timesaving double-grid technique

  J. R. Chelikowsky *et al.*, Phys. Rev. Lett. **72**, 1240 (1994).
  T. Ono and K. Hirose, Phys. Rev. Lett. **82**, 5016 (1999).
  K. Hirose and T. Ono, Phys. Rev. B **64**, 085105 (2001).
  T. Ono and K. Hirose, Phys. Rev. B **72**, 085105 (2005).
  T. Ono and K. Hirose, Phys. Rev. B **72**, 085115 (2005).

- Landauer formula with overbridging-boundary matching method

  M. Büttiker *et al.*, Phys. Rev. B **31**, 6207 (1985).
  Y. Fujimoto and K. Hirose, Phys. Rev. B **67**, 195315 (2003).
  T. Ono and K. Hirose, Phys. Rev. B **70**, 033403 (2004).

- Local-spin-density approximation and generalized gradient approximation

  J. P. Perdew and A. Zunger, Phys. Rev. B **23**, 5048 (1981).
  J. P. Perdew and Y. Wang, Phys. Rev. B **46**, 6671 (1992).

- Norm-conserving pseudopotential

  D.R. Hamann *et al.*, Phys. Rev. Lett. **43**, 1494 (1979).
  N. Troullier and J. L. Martins, Phys. Rev. B **43**, 1993 (1991).
  K. Kobayashi, Comput. Mater. Sci. **14**, 72 (1999). NCPS97

Background

Downsizing of electronic devices
Realization of nanoscale quantum devices

Nanoscale device

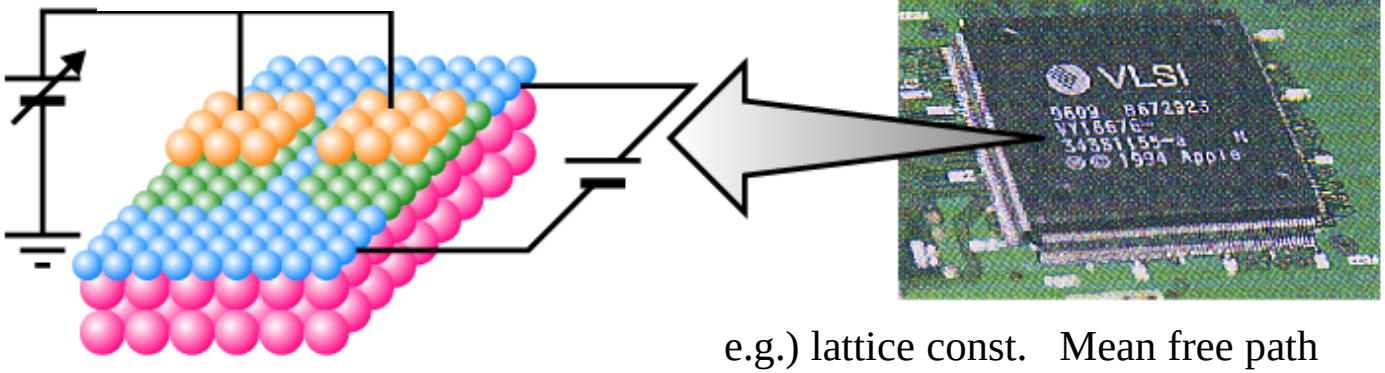

Dimensions << Mean free path

e.g.) lattice const. Mean free path

Si	5.428 Å	<<	~ 400 Å	(RT)
Au	4.078 Å	<<	~ 500 Å	(RT)

Regime where scattering due to lattice vibrations and defect is negligible

Electron transport ⇒ Ballistic
Quantum mechanical character of electrons

⇒ Observation of peculiar transport property

Analysis using theoretical and/or experimental approaches is urgent task to develop nanoscale devices!!

Scanning Tunneling Microscopy (STM)

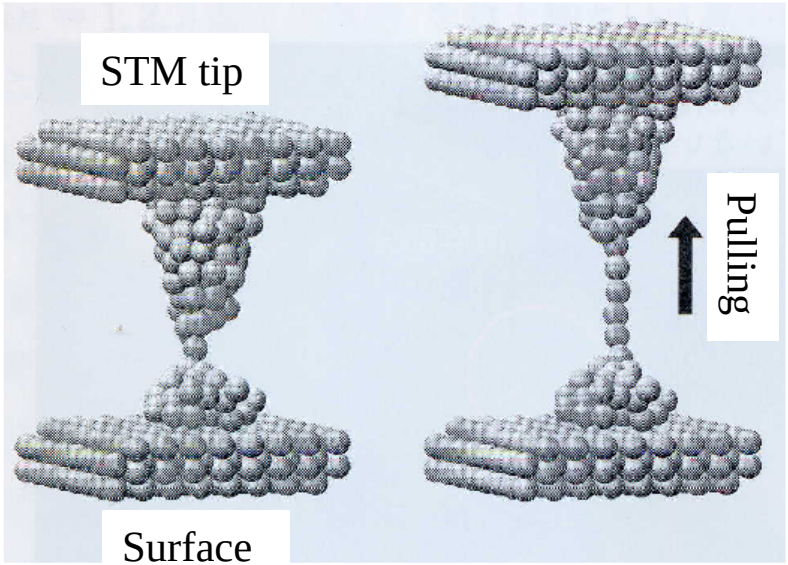

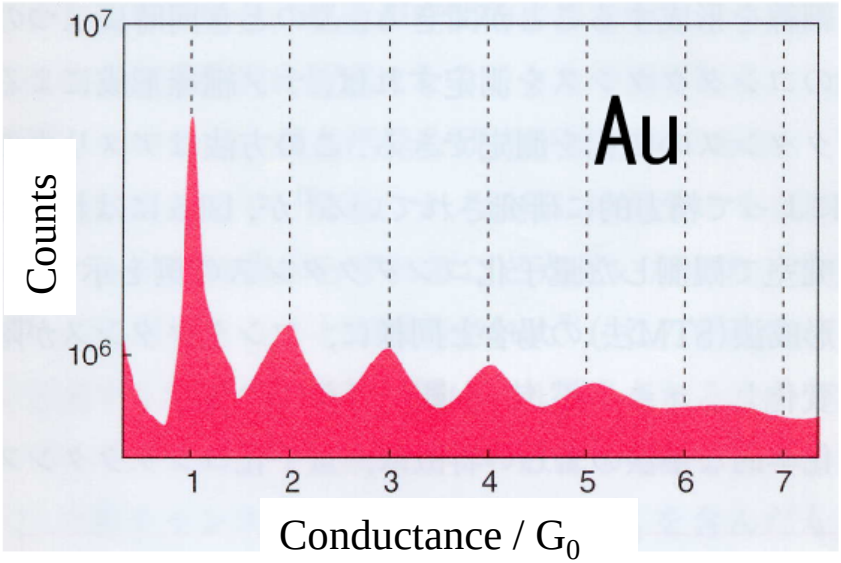

J.L.Costa-Kramer *et al.*,PRB **55**,12910(1997)

Unit of conductance quantization

$$G_0 = 2e^2/h$$

(*e*: electron charge, *h*: Plank's constant)

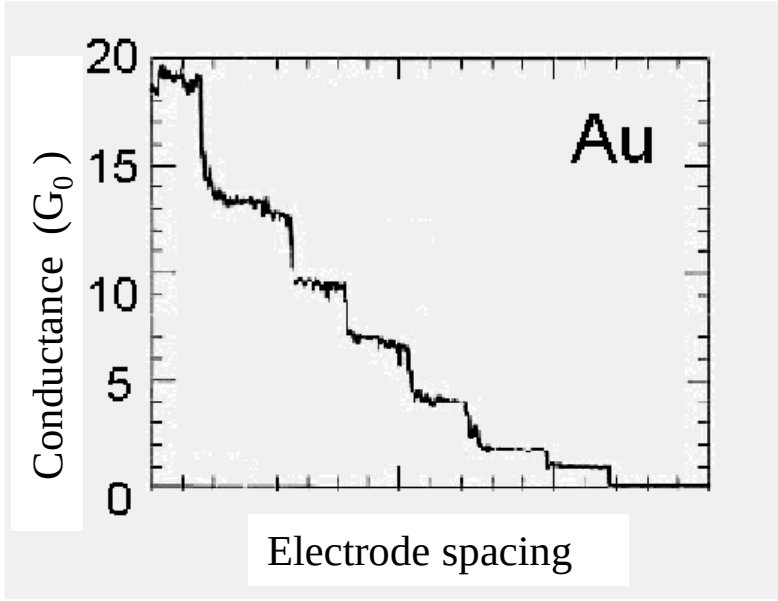

Rubio *et al.*,PRL **76** 2302 (1996)

Example of conductance quantization using mechanical controllable break junction

Transport properties of sodium nanowires

Computational Model

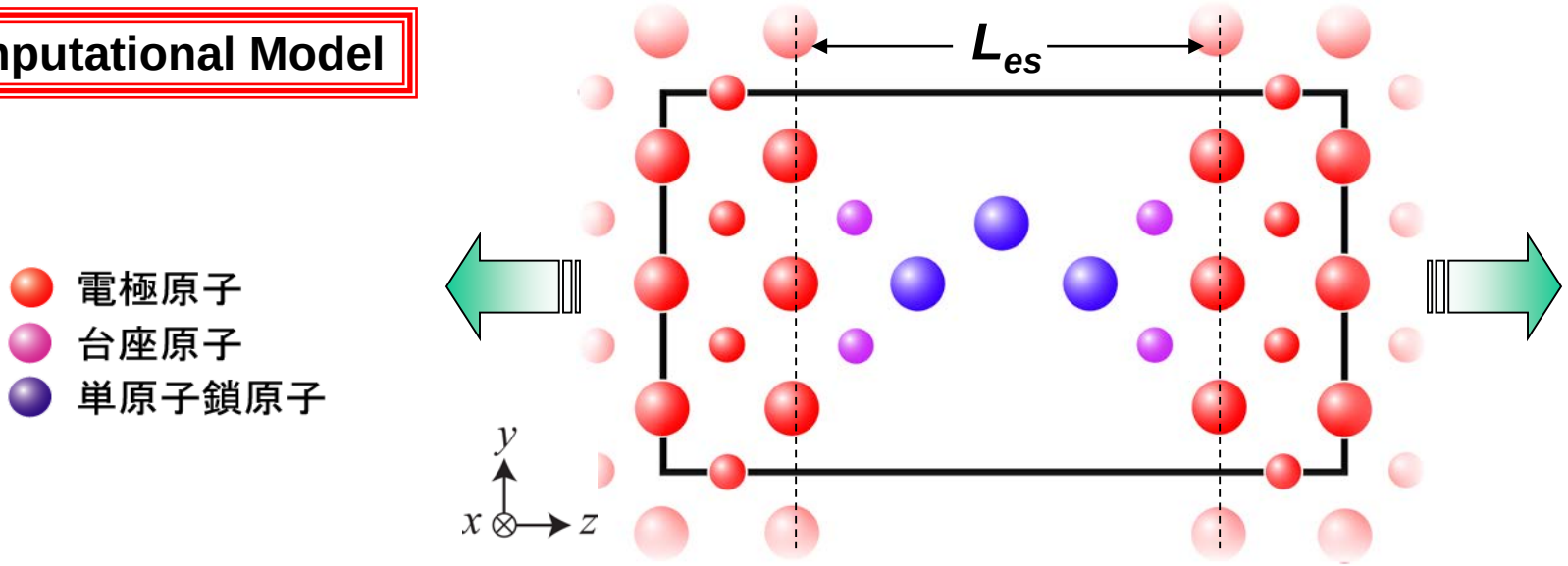

Variation of the conductance w.r.t. electrode spacing L_{es}

Quantized unit of conductance

$$G_0 = \frac{2e^2}{h}$$

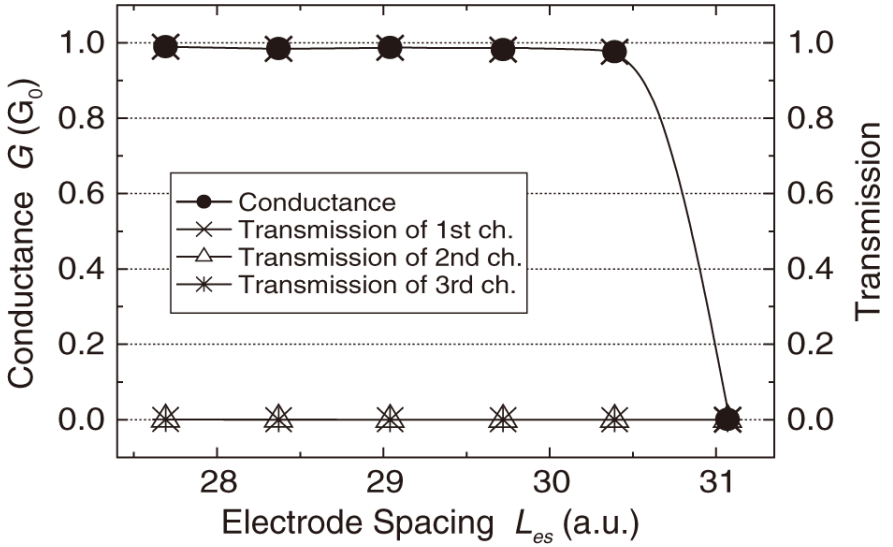

Y. Egami, T. Sasaki, T. Ono, and K. Hirose, Nanotechnology, **16**, S161 (2005).

Interest of electron transport calculations

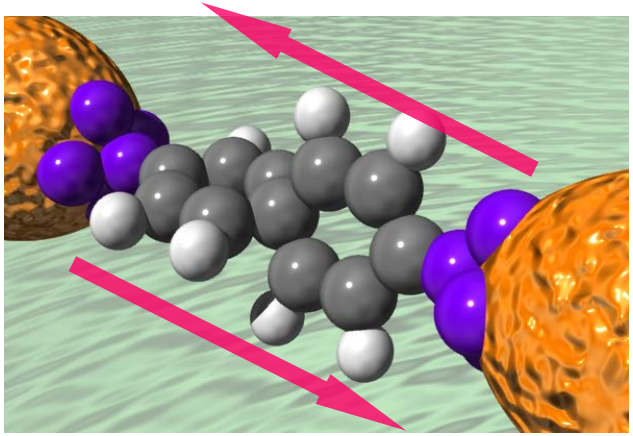

Electron transport through molecular chain suspended between electrodes

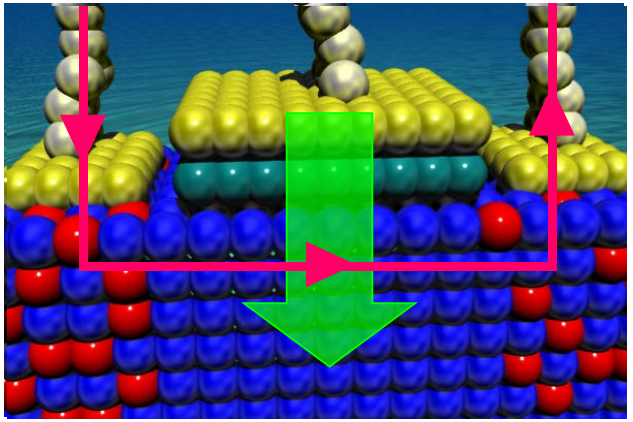

Electron transport between source and drain of semiconductor device

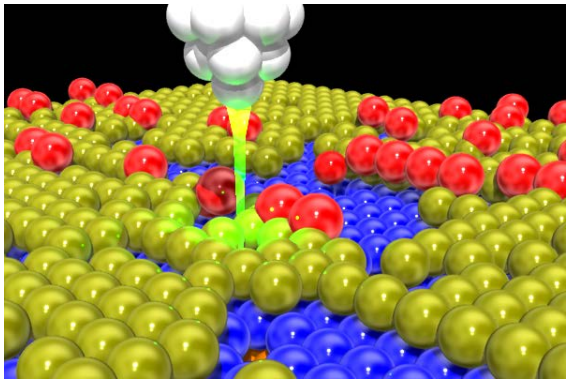

Tunneling current flowing between STM tip and sample surface

The ***understanding*** and ***control*** of the electron transport properties are **key subjects** for the development of new nanoscale devices.

Non-Equilibrium Green's Function method

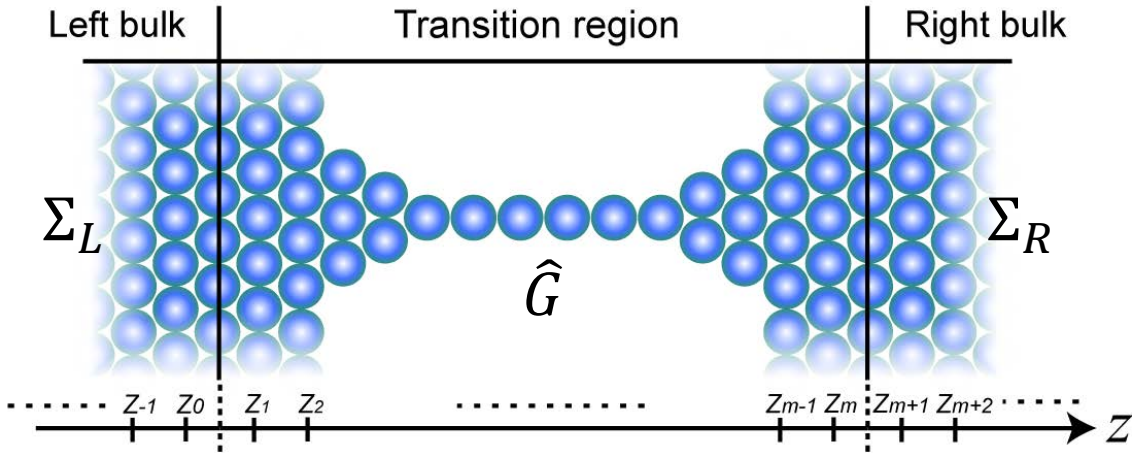

1. Compute self energy of electrodes $\hat{\Sigma}_{(L,R)}(Z)$, where Z is energy of electrons.

2. Compute perturbed (w/ electrodes) Green's function

$$\hat{G}(Z) = \left[Z - \hat{H} - \hat{\Sigma}_L(Z) - \hat{\Sigma}_R(Z)\right]^{-1}$$

where $\hat{H}$ is the Hamiltonian of the transition region.

For self-consistent calculation, charge density is calculated as $n(r) = -\frac{1}{\pi}\int \mathrm{Im}\,\hat{G}(Z)dZ$.

3. Compute conductance using Fisher-Lee formula.

$$\text{Conductance} = \frac{2e^2}{h}\mathrm{Tr}\left[\Gamma_L G^{r\dagger}\Gamma_R G^r\right]$$

$\Gamma_L = i\left[\Sigma_L^r - \Sigma_L^{r\dagger}\right]$ and $\Gamma_R = i\left[\Sigma_R^r - \Sigma_R^{r\dagger}\right]$ are coupling matrices.

Computations of $\hat{G}$ and Σ are time consuming!!

Difficulty in computing perturbed Green's functions

Perturbed Green's function includes electrode effect as Σ.

$$\hat{G} = \begin{bmatrix} E - A(z_0) - \Sigma_L(z_0) & -B & 0 & \cdots & & \cdots & 0 \\ -B\dagger & E - A(z_1) & -B & & & & \vdots \\ 0 & \ddots & \ddots & \ddots & & & \\ \vdots & & -B\dagger & E - A(z_l) & -B & & \vdots \\ & & & \ddots & \ddots & \ddots & 0 \\ \vdots & & & & -B\dagger & E - A(z_m) & -B \\ 0 & \cdots & & \cdots & 0 & -B\dagger & E - A(z_{m+1}) - \Sigma_R(z_{m+1}) \end{bmatrix}^{-1}$$

Load unbalance occurs due to the existence of solid matrices of Σs!

$$(zI - H - \Sigma_L - \Sigma_R)G = \begin{pmatrix} \Sigma_L & 0 & 0 \\ 0 & 0 & \Sigma_R \end{pmatrix} \begin{pmatrix} \\ \\ \\ \end{pmatrix}$$

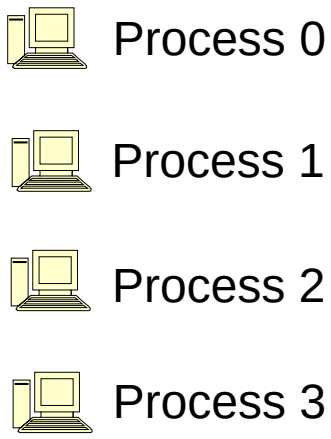

Vector elements are evenly distributed.

➡ Nonlinear equations & slow on massively parallel computers

Green's function in wave function matching method

Wave function matching uses unperturbed (w/o electrodes) Green's functions.
Effect of electrodes are included in wave function matching procedure.

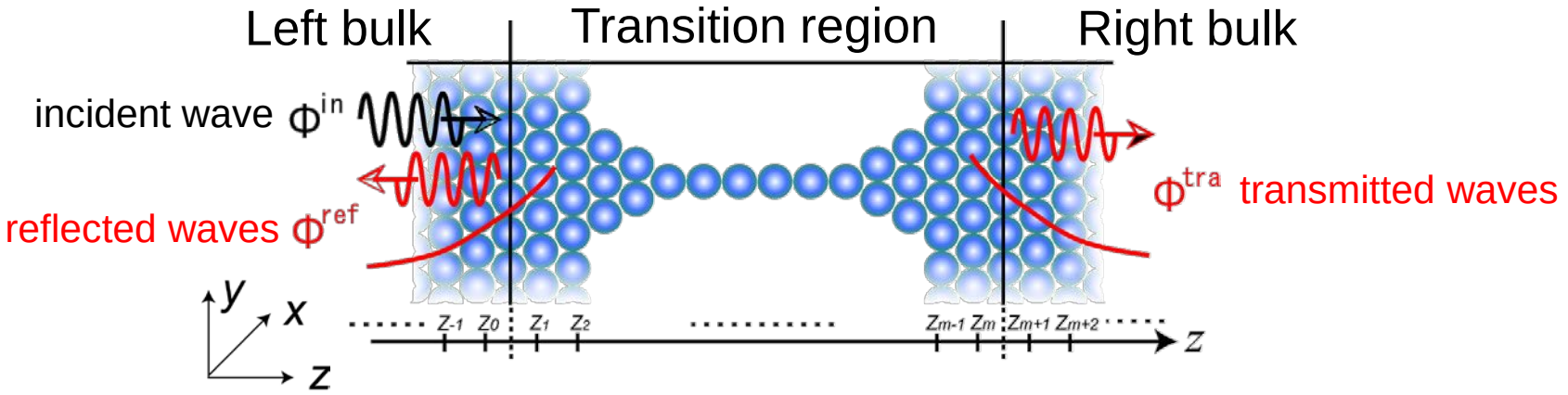

$(H - \varepsilon I)\psi_k = 0$ with ε being incident energy

$$G_{ij}(\varepsilon) := [\varepsilon I - H]^{-1}_{i,j} = (\boldsymbol{e}_i, \boldsymbol{x}_j) \ , \boxed{[\varepsilon I - H]\boldsymbol{x}_j = \boldsymbol{e}_j}$$

Shifted linear equations

Unperturbed Green' functions can be obtained very fast by shifted CG method!

Shifted CG method

Shifted CG method : use of the shift invariance of the Krylov subspace (**KS**)

R.Takayama *et. al.* Phys. Rev. B **73**, 165108 (2006)

$$K_n(A, \boldsymbol{b}) \coloneqq \mathrm{span}\{\boldsymbol{b}, A\boldsymbol{b}, \ldots, A^{n-1}\boldsymbol{b}\}$$

$$x^{\alpha}, x^{\beta} \in K_n(\varepsilon_{\alpha} I - H, \boldsymbol{e}_j) = K_n(\varepsilon_{\beta} I - H, \boldsymbol{e}_j)$$

The KS does not depend on the energy ε

Conventional CG

$(\varepsilon_1 I - H)\boldsymbol{x}^{(1)} = \boldsymbol{e}_j$ ← CG

⋮ ← CG

$(\varepsilon_k I - H)\boldsymbol{x}^{(k)} = \boldsymbol{e}_j$ ← CG

shifted CG

$(\varepsilon_1 I - H)\boldsymbol{x}^{(1)} = \boldsymbol{e}_j$ ← Store the KS

⋮ ← Reuse the KS for other energies

$(\varepsilon_k I - H)\boldsymbol{x}^{(k)} = \boldsymbol{e}_j$

The KS is constructed for each energy, which is time-consuming.

Algorithm of shifted CG method

$$A\boldsymbol{x} = \boldsymbol{b}$$

CG method

$$\boldsymbol{p}_n = \boldsymbol{r}_n + \beta_{n-1}\boldsymbol{p}_{n-1}$$

$$\alpha_n = \frac{\boldsymbol{r}_n^T \boldsymbol{r}_n}{\boldsymbol{p}_n^T A \boldsymbol{p}_n}$$

$$\boldsymbol{x}_{n+1} = \boldsymbol{x}_n + \alpha_n \boldsymbol{p}_n$$

$$\boldsymbol{r}_{n+1} = \boldsymbol{r}_n - \alpha_n A \boldsymbol{p}_n$$

$$\beta_n = \frac{\boldsymbol{r}_{n+1}^T \boldsymbol{r}_{n+1}}{\boldsymbol{r}_n^T \boldsymbol{r}_n}$$

matrix-vector product
vector-vector product

$\alpha, \beta, \boldsymbol{r}$

$$(A + \sigma I)\boldsymbol{x}^\sigma = \boldsymbol{b}$$

Shifted CG method

$$\pi_{n+1}^\sigma = R_{n+1}(-\sigma)$$

$$\alpha_n^\sigma = (\pi_n^\sigma / \pi_{n+1}^\sigma)\alpha_n$$

$$\beta_{n-1}^\sigma = (\pi_{n-1}^\sigma / \pi_n^\sigma)^2 \beta_{n-1}$$

$$\boldsymbol{p}_n^\sigma = 1/\pi_n^\sigma \, \boldsymbol{r}_n + \beta_{n-1}^\sigma \boldsymbol{p}_{n-1}^\sigma$$

$$\boldsymbol{x}_{n+1}^\sigma = \boldsymbol{x}_n^\sigma + \alpha_n^\sigma \boldsymbol{p}_n^\sigma$$

scalar-vector product

Computationally moderate!

But, this method is applicable only for linear equations.

Advantage of computing unperturbed Green's functions

Unperturbed Green's function does not include electrode effect.

$$\hat{g} = \begin{bmatrix} E - A(z_0) & -B & & & & 0 \\ -B^{\dagger} & E - A(z_1) & -B & & & \\ & \ddots & \ddots & \ddots & & \\ & & \ddots & \ddots & \ddots & \\ & & & -B^{\dagger} & E - A(z_m) & -B \\ 0 & & & & -B^{\dagger} & E - A(z_{m+1}) \end{bmatrix}^{-1}$$

Load unbalance does not happen.

$$(zI - H)g = \begin{pmatrix} & & 0 \\ & & \\ 0 & & \end{pmatrix} \begin{pmatrix} \\ \\ \\ \end{pmatrix}$$


Process 0


Process 1


Process 2


Process 3

Shifted linear equations & fast on massively parallel computers

Relation between perturbed and unperturbed GFs

Dyson's equation in the standard form is

$$\begin{bmatrix} G_{0,l} \\ G_{1,l} \\ \vdots \\ G_{l,l} \\ \vdots \\ G_{m,l} \\ G_{m+1,l} \end{bmatrix} = \begin{bmatrix} g_{0,0} & g_{0,1} & \cdots & g_{0,m} & g_{0,m+1} \\ g_{1,0} & g_{1,1} & \cdots & g_{1,m} & g_{1,m+1} \\ \vdots & \vdots & & \vdots & \vdots \\ & & & & \\ \vdots & \vdots & & \vdots & \vdots \\ g_{m,0} & g_{m,1} & \cdots & g_{m,m} & g_{m,m+1} \\ g_{m+1,0} & g_{m+1,1} & \cdots & g_{m+1,m} & g_{m+1,m+1} \end{bmatrix} \begin{bmatrix} \Sigma_L(z_0)G_{0,l} \\ 0 \\ \vdots \\ I \\ \vdots \\ 0 \\ \Sigma_R(z_{m+1})G_{m+1,l} \end{bmatrix} \leftarrow l \text{ th row}$$

Here, $g_{k,l}$ is kth block line and lth block row of $\hat{g}$.

From 0 th, l th, and $m+1$ th block rows, we have

$$\begin{pmatrix} g_{0,0}\Sigma_L(z_0) - I & g_{0,m+1}\Sigma_R(z_m) \\ g_{m+1,0}\Sigma_L(z_1) & g_{m+1,m+1}\Sigma_R(z_m) - I \end{pmatrix} \begin{pmatrix} G_{0,l} \\ G_{m+1,l} \end{pmatrix} = -\begin{pmatrix} g_{0,l} \\ g_{m+1,l} \end{pmatrix}.$$

By solving the above equations, we obtain the relation between perturbed Green's function G and unperturbed Green's function g.

$$G_{1,1} = \tilde{g}_{1,1}\left[I - \Sigma_L(z_1)\tilde{g}_{1,1}\right]^{-1} \text{ with } \tilde{g}_{1,1} \text{ being } g_{1,1} + g_{1,m}\Sigma_R(z_m)\left[I - g_{m,m}\Sigma_R(z_m)\right]^{-1} g_{m,1} \ .$$

Proof is in T. Ono *et al.*, PRB 86 195406 (2012).

Effect of shifted CG method

Collaboration with Prof. Cho (Nagoya U.) and Prof. Hoshi (Tottori U.)

Computational model (Na nanowire)

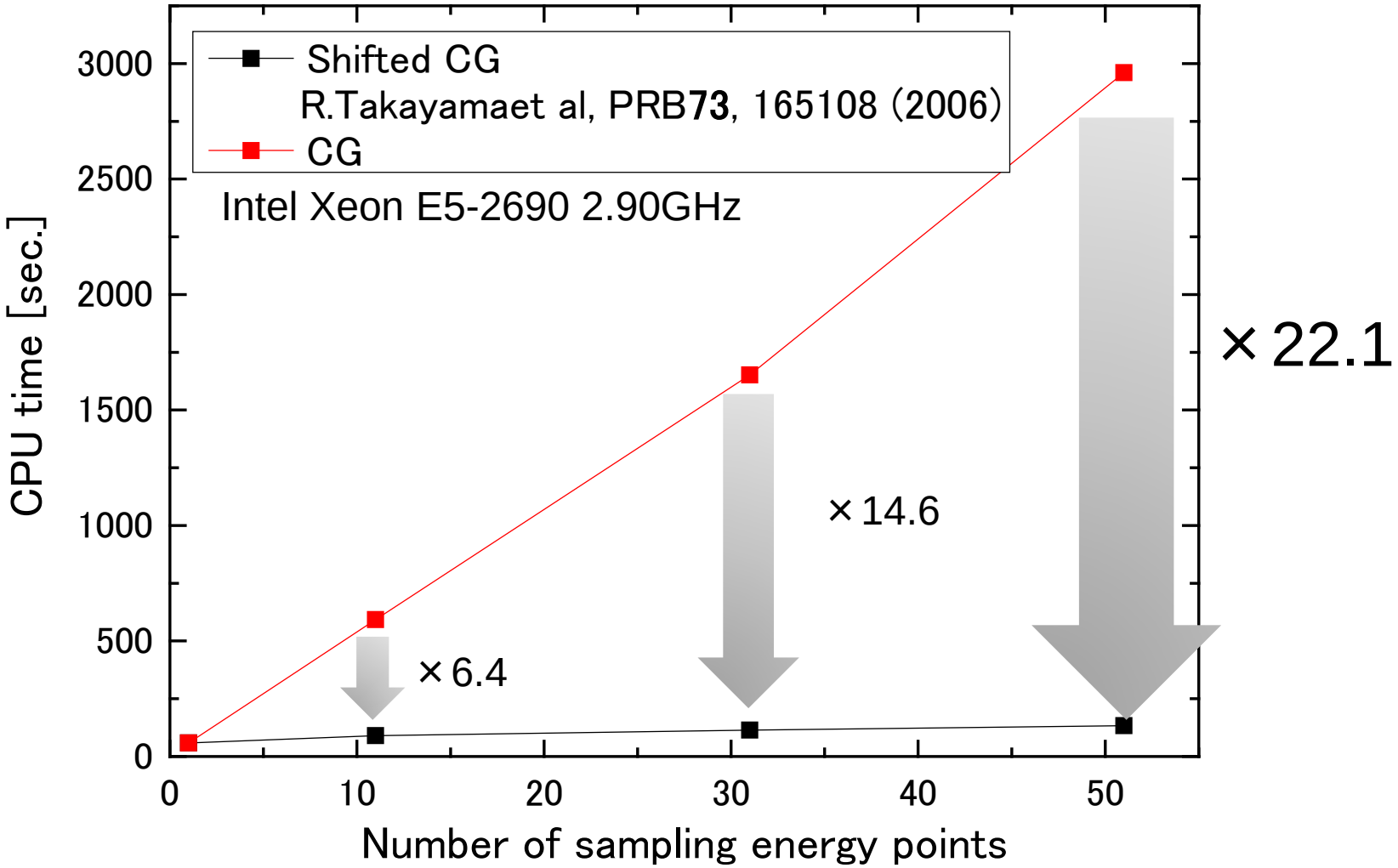

Shifted CG becomes powerful as the number of sampling points increases!

Power Transmission

Power devices

Electronic devices for AC-DC, voltage, and frequency conversions.

Resource and energy problem

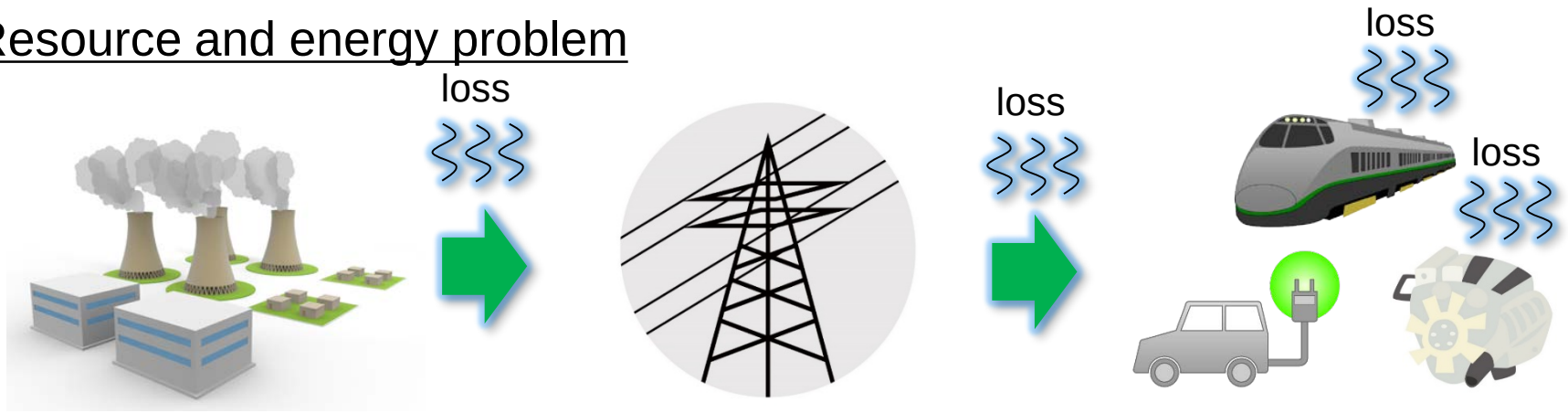

10% of electronic power is lost as heat
(10%=80TeraWh/year)

Development of low loss power conversion devices is indispensable.

Technological limit of Si-based power devices is approaching
because the band gap of Si is small for power devices.

SiC is one of the promising candidates to replace Si!

Problems of SiC-based MOSFET

Low carrier mobility

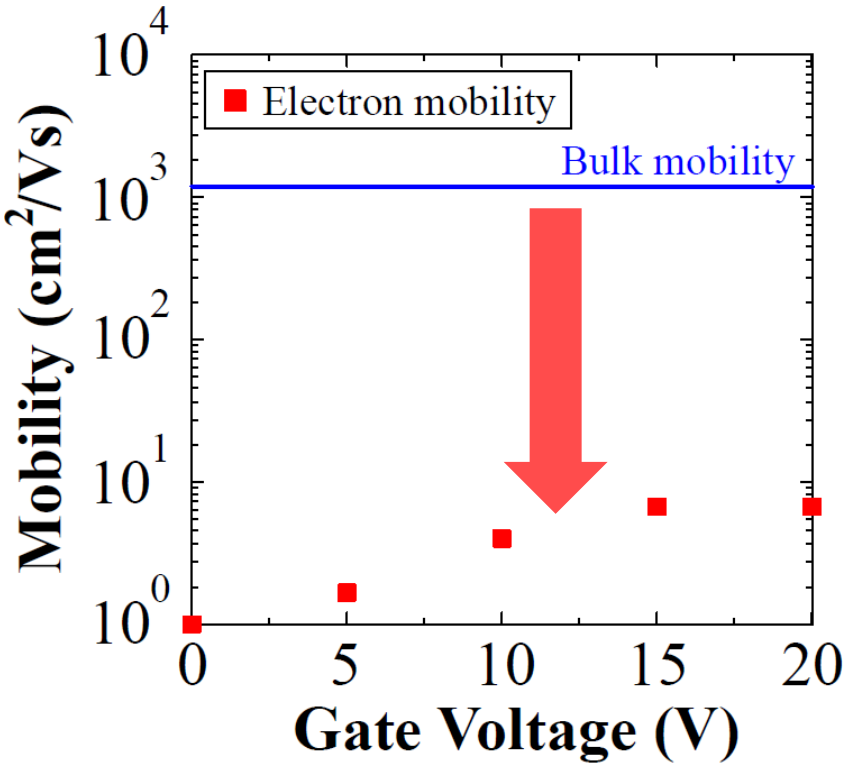

Data taken from D. Okamoto *et al.*, IEEE EDL **31** 710 (2010).

Threshold voltage shift

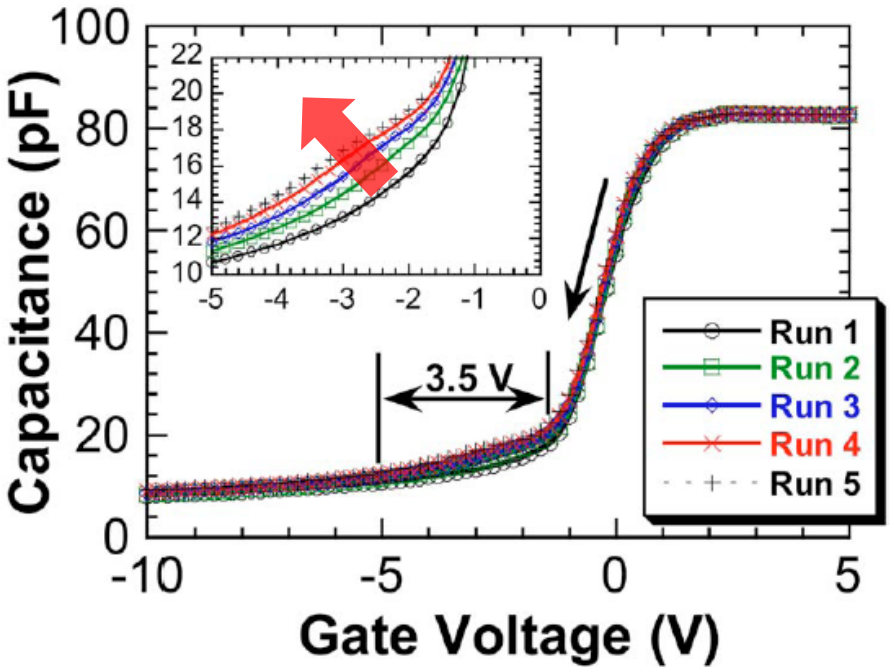

MJ Marinella *et al.*, APL **90** 253508 (2007).

These problems are believed to be caused by interface defects near SiC/SiO_2 interface.

It is of importance to study the oxidation process of SiC.

Thermal oxidation of SiC

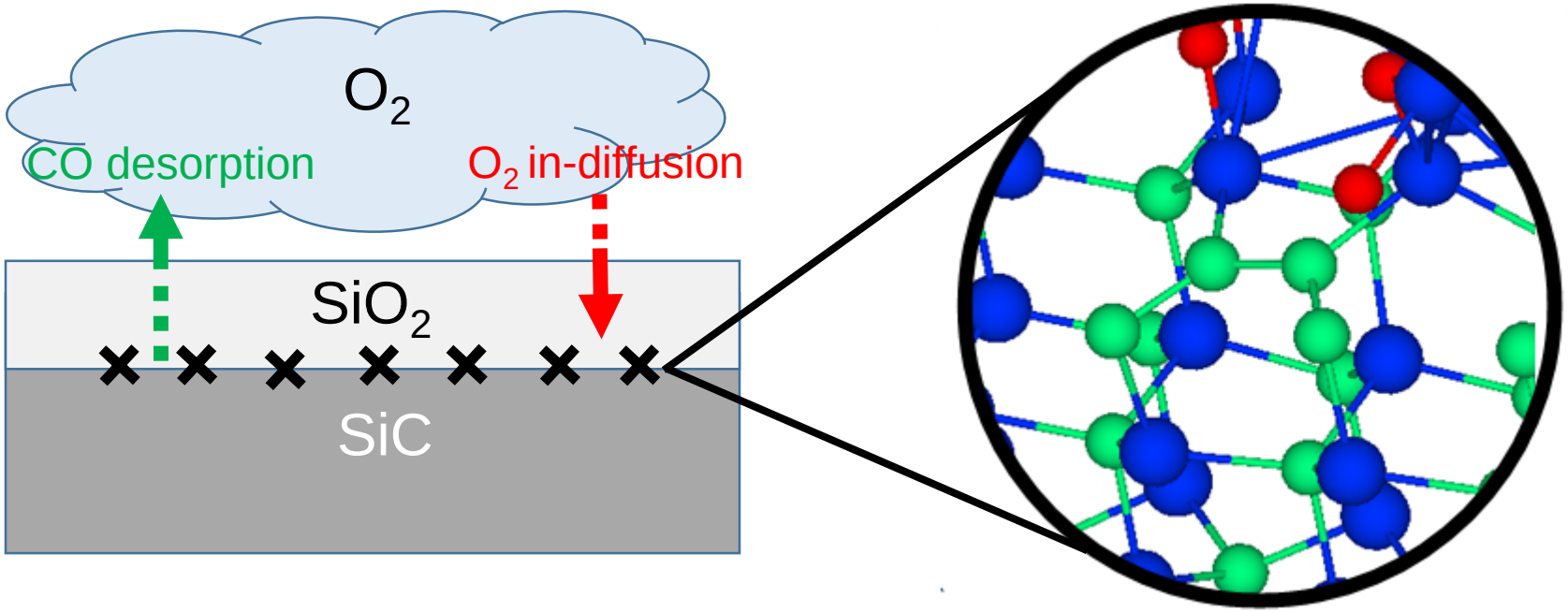

There may exist various C- and O-related defects at the interface, but their effect on carrier mobility is not clear.

Purpose of this study is

To clarify the relationship between interface atomic structures and carrier-scattering properties.

Computational method & model

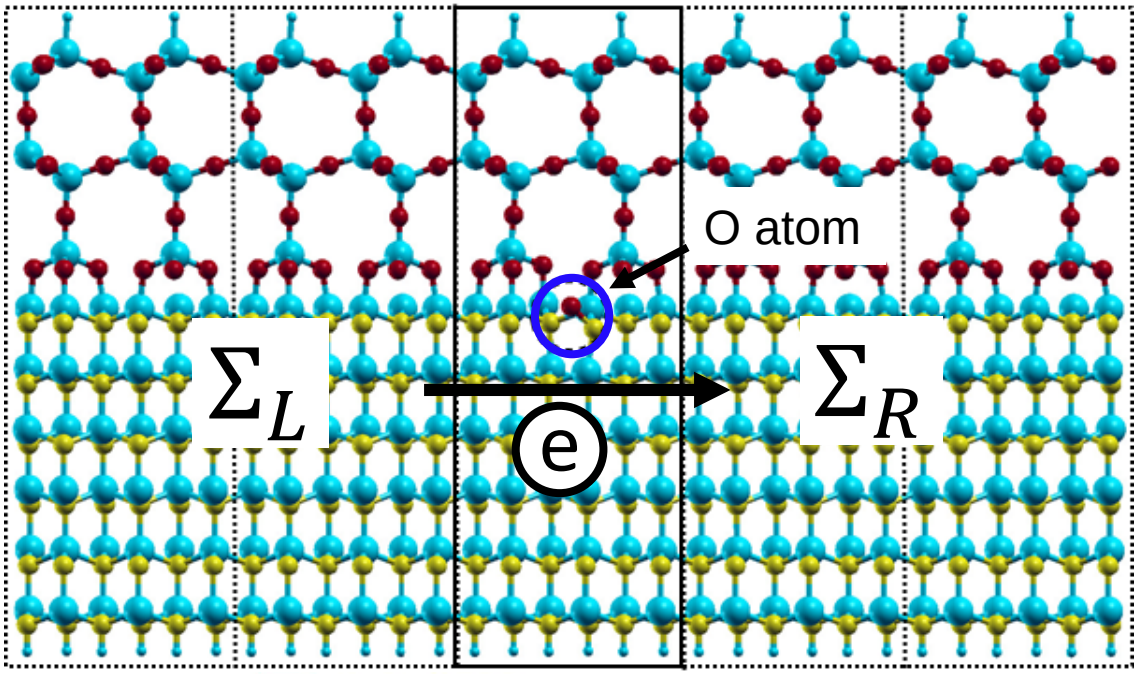

Optimization

Transport Calculation

RSPACE code is employed

Density Functional Theory

Real-space finite-difference

Projector augmented wave (PAW)

Local density approximation (LDA)

T. Ono *et al*, PRB **82**, 205115 (2010)

NEGF-Landauer method

$$T(E) = \mathrm{Tr}[\hat{\Gamma}_L \hat{G}^r \hat{\Gamma}_R \hat{G}^{r\dagger}]$$

$$I(V) = \frac{2e}{h} \int_{\mu_R}^{\mu_L} dE\, T(E)$$

T. Ono *et al*, PRB **86**, 195406 (2013)

S. Iwase *et al*, PRE **91**, 063305 (2015)

Two types of surface & interface

4H-SiC(0001) has stacking sequence of ABCBAB…. shows two types of surface.

AFM image

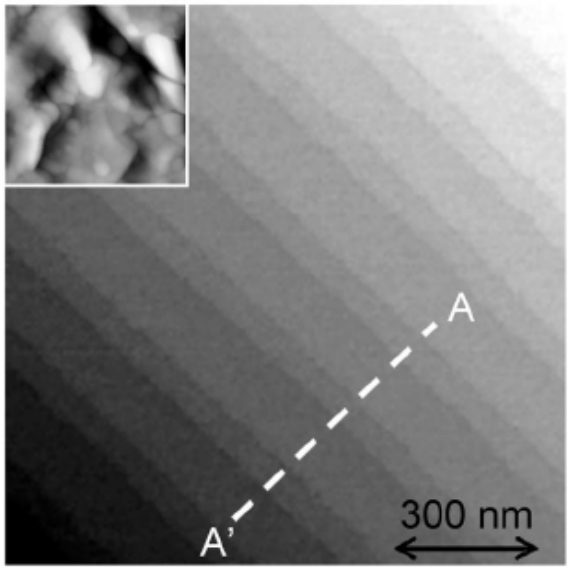

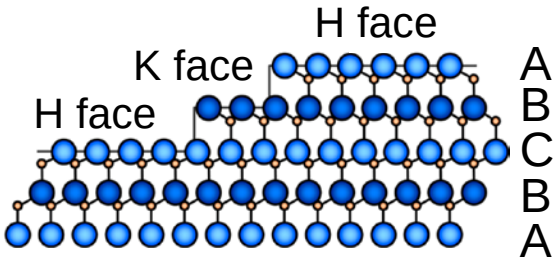

K. Arima et al, APL 90 202106 (2009)

Interface models

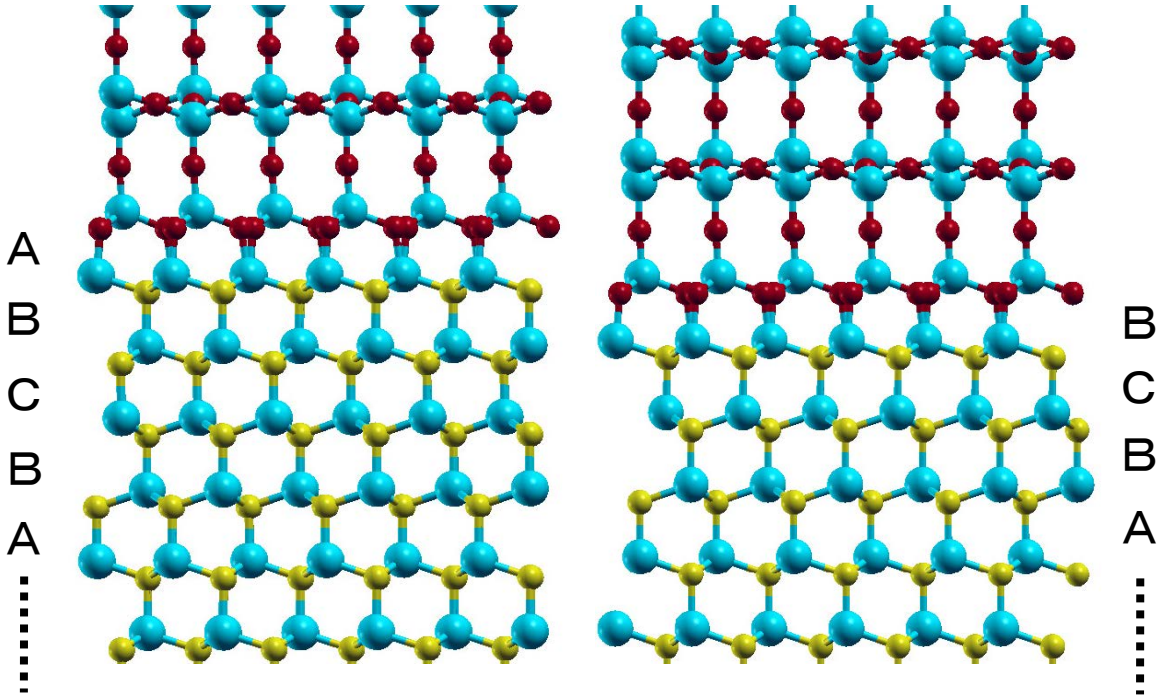

Cubic(K) interface

Hexagonal(H) interface

Interface atomic structures during thermal oxidation

Thermal oxidation of 4H-SiC(0001) undergoes as following steps.

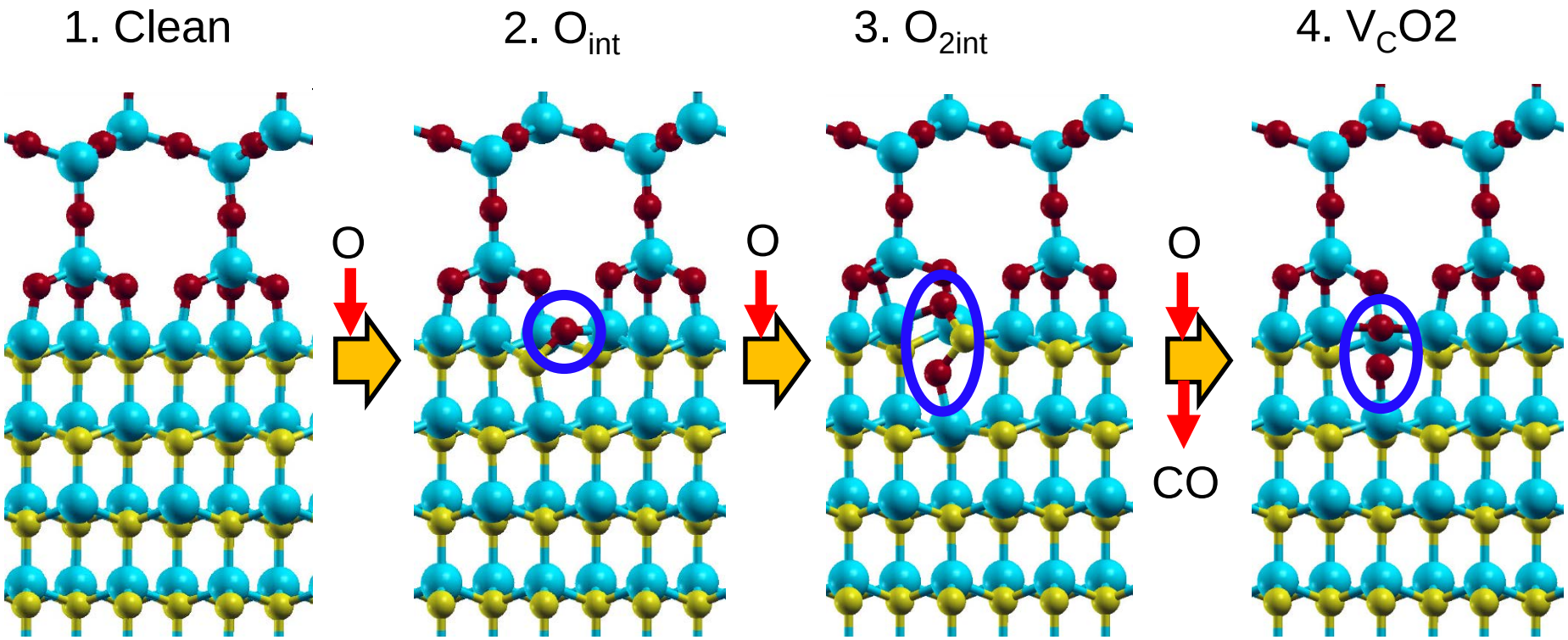

Carrier scattering properties of above 4 models are examined for K and H interfaces.

I-V curve

K interface

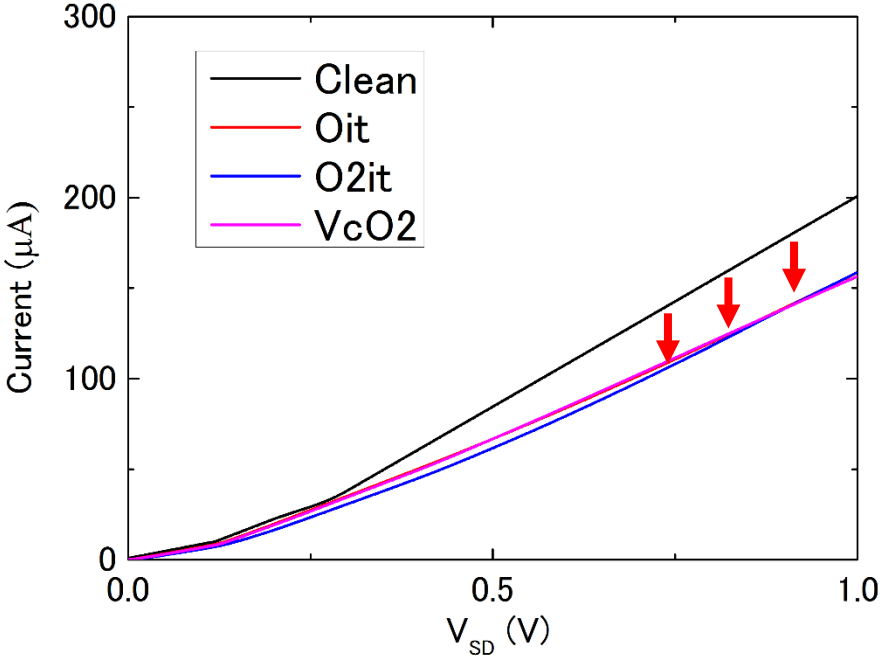

H interface

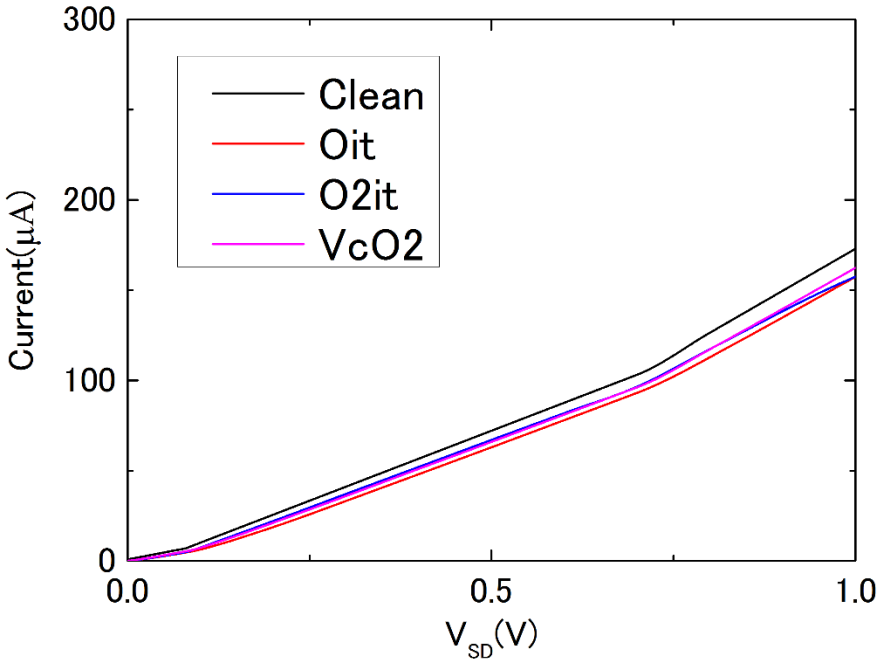

- C interface is more sensitive to the insertion of O atoms than H interface.
- Just single inserted O atom at K interface reduces conductance!

Conduction band edge states of SiC

Si

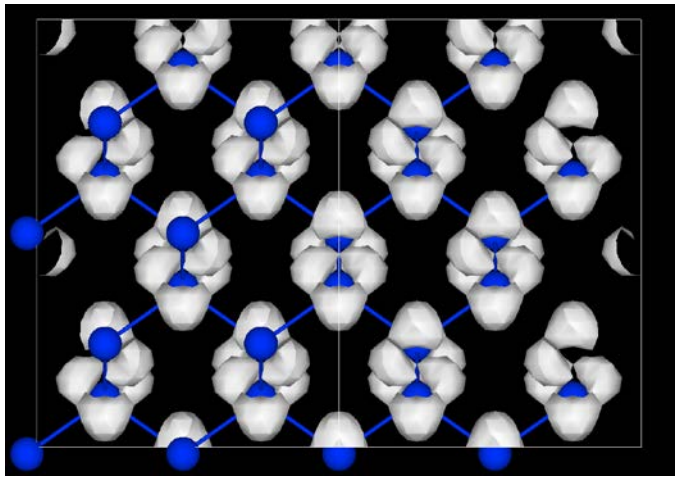

- sp^3 anti-bonding state
- Localized around Si atoms

SiC

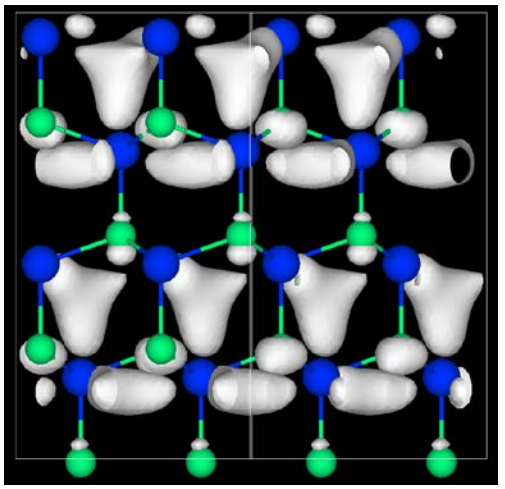

- Nearly free electron (NFE) like
  Y. Matsushita et al., PRL108 246404 (2012).
- Accumulating at inter layer
- Easily affected by stacking sequence

- Stacking sequence of SiC affects the behavior of the NFE states at the interface.
- Control of the NFE states is an important issue to improve the carrier mobility of SiC-MOSFET!

Summary

Development of RSPACE code

- As the progress of parallel computers, the real-space methods for first-principles calculations are developed.
- With this stream, RSPACE has been developed.
- Electronic current in nanoscale systems is quite different from that in macro scale systems. Although it is difficult for the conventional methods to examine this phenomena, RSPACE can investigate owing to the flexibility of boundary conditions.
- Computation of the perturbed Green's function is one of the bottle necks in transport calculations. We have overcome by the shifted CG method and good scalability of the real-space method.

Application(Carrier scattering property of SiC-MOS interface)

- Low carrier mobility at SiC/SiO_2 hampers the realization of SiC-MOSFET. To improve the mobility, control of the NFE states lying the conduction band edge is important.